HHS Public Access

Author manuscript

Mol Psychiatry. Author manuscript; available in PMC 2019 October 26.

Published in final edited form as:

Mol Psychiatry. 2019 November ; 24(11): 1696–1706. doi:10.1038/s41380-018-0062-0.

Elevated levels of brain homocysteine directly modulates the pathological phenotype of a mouse model of tauopathy

Antonio Di Meco, M.Sci[1], **Jian-Guo Li, PhD**[1], **Carlos Barrero, PhD**[2], **Salim Merali, PhD**[2], **Domenico Praticò, MD**[1]

[1]Alzheimer's Center at Temple, Lewis Katz School of Medicine, Temple University, Philadelphia PA, 19140

[2]Department of Pharmaceutical Sciences, Temple University, Philadelphia PA, 19140

Abstract

High circulating level of homocysteine (Hcy), also known as hyper-homocysteinemia, is a risk factor for Alzheimer's disease (AD). Previous studies showed that elevated Hcy promotes brain amyloidosis and behavioral deficits in mouse models of AD. However, whether it also directly modulates the development of tau neuropathology independently of amyloid-beta in vivo is unknown. Herein we investigate the effect of diet-induced elevated levels of brain Hcy on the phenotype of a relevant mouse model of human tauopathy. Compared with controls, tau mice fed low folate and B vitamins diet, had a significant increase in brain Hcy levels and worsening of behavioral deficits. The same mice had a significant elevation of tau phosphorylation, synaptic pathology and astrocytes activation. In vitro studies demonstrated that Hcy effect on tau phosphorylation was mediated by an upregulation of the 5-lipoxygenase via cdk5 kinase pathway activation. Our findings support the novel concept that high Hcy levels in the central nervous system is a metabolic risk factor also for neurodegenerative diseases specifically characterized by the progressive accumulation of tau pathology, namely tauopathies.

INTRODUCTION

Besides amyloid beta (Aβ) peptides deposition, the accumulation of intracellular aggregates of hyper-phosphorylated microtubule associated protein tau is the second principal hallmark feature of Alzheimer's disease (AD) (1, 2). Interestingly, this very type of neuropathology characterizes other neurodegenerative disorders, which for this reason are called tauopathies. Among them, Progressive Supranuclear Palsy, Pick's disease, and Cortico-basal

Correspondence to: Domenico Praticò, MD, 3500 North Broad Street, MERB, 947, Philadelphia, PA 19140, Tel: 215-707-9380, Fax: 215-707-9890, praticod@temple.edu.

AUTHORS' CONTRIBUTIONS

A.D.M. and D.P. designed the study; A.D.M. and J.G.L. performed the experiments; C.B. and S.M. were involved in the measurement of Hcy SAM an SAH; A.D.M. and D.P. analyzed the data and drafted the manuscript. All authors have discussed the results and seen the final version of the paper before submission.

CONFLICT OF INTEREST

The authors declare no conflict of interest.

degeneration are probably the most common and most investigated (3). Since the majority of tauopathies are sporadic and no precise etiological factors have been identified, emerging data support the hypothesis that a combination of genetic and environmental risk factors by interacting with each other could ultimately be responsible for the onset of these diseases (4). High circulating levels of homocysteine, also known as hyper-homocysteinemia (HHcy), is a known modifiable risk factor for AD independently from other variables (5, 6). Studies performed in animal and cellular models of AD demonstrated that HHcy modulates both Aβ and tau metabolism (7–10). However, no data are available on the direct effect of high Hcy levels on tau phosphorylation and related neuropathology in a mouse model of pure tauopathy devoided of any Aβ pathology.

Recently, we have demonstrated that HHcy promotes upregulation of the 5-Lipoxygenase (5LO) enzymatic pathway in the brain of an AD mouse model and in AD cell model through a de-methylation-dependent effect on its promoter, and that this is functional importance for the development of their amyloidotic phenotype (11). However, whether high Hcy can also specifically affect in vivo tau phosphorylation and neuropathology via a 5LO-dependent activation mechanism remains to be investigated.

For this reason in the current studies, we tested the effect of brain high Hcy levels on the development of tau pathology in a relevant tau transgenic mouse model, the human tau (h-tau) mouse (12). We reached this goal by a chronic dietary approach known to induce a significant increase in Hcy *in vivo* and then assessed its effect on learning and memory, tau phosphorylation, synaptic integrity and neuroinflammation in this model.

MATERIALS and METHODS

Animal and treatments

All animal procedures were approved by the Animal Care and Usage Committee, in accordance with the U.S. National Institutes of Health guidelines. The h-tau mice used in this study have been already fully described and characterized (12). At the beginning of the study, mice were randomized to two groups. The control CTR group mice (n = 8 [4 males and 4 females]) were given the standard rodent chow, whereas the DIET group mice (n = 10 [5 males and 5 females]) a standard rodent chow deficient in folate (<0.2 mg/kg), vitamin B6 (<0.1 mg/kg) and B12 (<0.001 mg/kg), which is known to induce HHcy in mice (13). The diets were custom-made, prepared by a commercial vendor (Harlan Teklad, Madison, WI), and always matched for calories.

Starting at 4 months of age, mice received the diets for 8 months until they were 12 month-old. A separate group of animals was later randomized to receive regular chow (CTR) (n = 7 [3 males and 4 females]) or the DIET (n = 9 [4 males and 5 females]) from 4 to 8 months of age. During the study, mice in both groups gained weight regularly, and no significant differences in weight were detected between the two groups by the end of the study (data not shown). No macroscopic effect on the overall general health was observed in the animals receiving the DIET when compared with control group. No macroscopic differences were observed when at sacrifice we compared major organs such as liver, spleen, heart and kidneys between the 2 groups. After euthanasia, brains were removed and dissected in two

halves by a mid-sagittal dissection: one for biochemistry assays, the other for immunohistochemistry studies.

Behavioral tests

All animals were always pre-handled for 2–3 days prior testing. They were assessed in a randomized order by an experimenter blinded to the treatment.

Y-maze

The Y-maze apparatus consisted of three arms 32 cm (long) 610 cm (wide) with 26-cm walls (San Diego Instruments, San Diego, CA). Testing was always performed in the same room and at the same time to ensure environmental consistency as previously described (14,15).

Morris water maze

Briefly, the apparatus used was a white circular plastic tank (122 cm in diameter), filled with water maintained at room temperature, which was made opaque by the addition of a nontoxic white paint, and inside had a removable, square (10 cm in side length) plexiglass platform. The tank was located in a test room containing various prominent visual cues. Mice were trained to swim to the platform submerged 1.5 cm beneath the surface of the water and invisible to the mice while swimming. The platform was located in a fixed position, equidistant from the center and the wall of the tank. Mice were subjected to four training trials per day (inter-trial interval, 15 minutes). During each trial, mice were placed into the tank at one of four designated start points in a random order. Mice were allowed to find and escape onto the submerged platform. If they failed to find the platform within 60 seconds, they were manually guided to the platform and allowed to remain there for 10 seconds. Mice were trained to reach the training criterion of 20 seconds (escape latency). They were assessed in the probe trial 24 hours after the last training session, which consisted in a 60-second free swim in the pool without the platform. Each animal's performance was recorded for the acquisition parameters (latency to find the platform) and the probe-trial parameters (number of entries to the platform and time in quadrants) (14,15).

Cell line and treatment

Neuro-2 A neuroblastoma (N2A) cells stably expressing YFP-tagged human tau cDNA (N2A-tau) driven by the CMV promoter were prepared in house, as previously described (16). Cells were cultured in Dulbecco's modified Eagle medium supplemented with 10% fetal bovine serum, 100 U/mL streptomycin (Cellgro, Herdon, VA) and 100 mg/mL Hygromycin B (Invitrogen, Carlsbad, CA) at 37°C in the presence of 5% CO_2 as previously described (17). The cells were cultured to 80% to 90% confluence in six-well plates and then changed to fresh medium containing 50 μM DL-homocysteine (Sigma, St Louis, MO), 40μM adenosine (Sigma, St. Louis, MO), and 10μM erythro-9-(2-hydroxy-3-nonyl)-adenine hydrochloride (Sigma, St. Louis, MO), or 100 μM zileuton (Sigma, St Louis, MO), as previously described (11, 13). After 24 hrs, cell lysates harvested and protein extracts used for Western blotting analyses.

Biochemical analyses

Brain tissues were homogenized and sequentially extracted in RIPA and then formic acid (FA), where the RIPA fraction contains the soluble, whereas the FA fraction the insoluble form of tau protein, as previously described (13–17). Levels of Hcy, S-adenosyl-homocysteine (SAH) and S-adenosyl-methionine (SAM) in brain tissue were assayed by high-performance liquid chromatography, as previously described (18). LTB4 levels were assayed by a specific and sensitive enzyme linked immunosorbent assay kit (Assay Designs Inc., Ann Arbor, MI), following the manufacturer's instruction and as previously described (19,20).

Western Blot Analyses

RIPA fractions of brain homogenates were used for Western blot analyses as previously described (13–17). Briefly, samples were electrophoresed on 10% Bis–Tris gels or 3–8% Tris–acetate gel depending on the molecular weight of the protein of interest (Bio-Rad, Richmond, CA), transferred onto nitrocellulose membranes (Bio-Rad, Richmond, CA), and then incubated overnight with the appropriate primary antibodies as indicated in the Table. After three washings, membranes were incubated with IRDye 800CW-labeled secondary antibodies (LI-COR Bioscience, Lincoln, NE) at room temperature for 1 hr. Signals were developed with Odyssey Infrared Imaging Systems (LI-COR Bioscience, Lincoln, NE). β-actin was used as internal loading control.

Quantitative Real Time RT-PCR

RNA was extracted and purified using the RNeasy mini-kit (Qiagen, Valencia, CA), as previously described (20,21). Briefly, 1μg of total RNA was used to synthesize cDNA in a 20μl reaction using the RT2 First Strand Kit for RT-PCR (SuperArray Bioscience, Frederick, MD). The 5LO gene was amplified by using commercially available primers for Alox5 (Qiagen, Valencia CA, cat # PPM28755C). β-Actin gene was amplified by using commercially available primers (Qiagen, Valencia CA, cat # PPM02945B) and used as an internal control gene to normalize for the amount of RNA. Quantitative real-time RT-PCR (qRT-PCR) was performed by using StepOnePlus Real-Time PCR Systems (Applied Biosystems, Foster City, CA). Two microliters of cDNA was added to 10μl of SYBR Green PCR Master Mix (Applied Biosystems, Foster City, CA). Each sample was run in duplicate, and analysis of relative gene expression was done by StepOne software v2.1.

Immunohistochemistry

Immunostaining was performed as described in our previous studies (13–17). Briefly, serial coronal sections were mounted on 3-aminopropyl triethoxysilane (APES)-coated slides. Every eighth section from the habenular to the posterior commissure (6–8 sections per animal) was examined using unbiased stereological principles. Sections used for testing HT7, PHF13, AT180, synaptophysin, PSD95 and MAP2 were deparaffinized, hydrated and subsequently with 3% H_2O_2 in methanol, and then antigen retrieved with 10 mM sodium citrate buffer. Sections were blocked in 2% fetal bovine serum before incubation with the appropriate primary antibody overnight at 4°C. After washing, sections were incubated with biotinylated anti-mouse IgG (Vector Lab, Burlingame, CA) and then developed by using the

avidin-biotin complex method (Vector Lab, Burlingame, CA) with 3,3′-diaminobenzidine (DAB) as a chromogen. Light microscopic images were captured using software QCapture 2.9.13 (Quantitation Imaging Corporation, Surrey, Canada) with the auto-exposure option. These images were used to calculate the area occupied the immunoreactivities using the software Image-ProPlus (Media Cybernetics).

Data Analysis

Data analyses were performed using Graphpad Prism for Windows version 5.00. Statistical comparisons were performed by Unpaired Student's t-test or one way Anova test for experiments including more than two groups. Values in all figures and table represent mean ± S.E.M. Significance was set at $p<0.05$.

RESULTS

Diet low in folate and B vitamins promotes behavioral deficits in h-tau mice

To investigate the effect of a low folate and B vitamins diet on cognition, CTR and DIET mice were assessed in the Y-maze and the Morris water maze test at 12 months of age. No significant differences were observed between the two groups of mice in the Y-maze test for the number of entries as well as percentage of alternations (Figure 1A, B). In the Morris water maze, no differences were noted in the average swimming speed and the cued phase of the test between the two groups of mice (Figure 1C, E). However, in the training phase DIET-receiving animals learned the platform position significantly slower compared to CTR mice (Figure 1D). In addition, mice on the DIET showed a significant decrease in the number of entries in the platform zone and time spent in the platform zone compared to CTR, as well as a trend towards increase in the time spent in the opposite zone compared to CTR (Figure 1F–H). No significant differences were observed when males and females in each group were analyzed separately for both paradigms (data not shown).

Diet-induced elevated homocysteine worsens tau neuropathology in h-tau mice

First, we wanted to confirm compliance with the dietary regimen chronically administered to the mice by assessing levels of Hcy in their central nervous system. As shown in figure 2, h-tau mice receiving the diet had a statistically significant increase in levels of homocysteine (Hcy), and S-adenosyl-homocysteine (SAH), and a reduction in the levels of S-adenosyl-methionine (SAM) which did not reach statistical significance. However, we observed that the same mice had a significant reduction in the ratio of SAM/SAH (Figure 2A).

Next, brain homogenates from the two groups of mice were assessed for levels of total soluble tau protein and its phosphorylated isoforms at specific epitopes by Western blot and immunohistochemistry. Compared with controls, h-tau mice receiving the DIET showed a significant increase in tau phosphorylation at Thr231/Ser235 and Ser396, as recognized by AT180 and PHF13 antibodies, respectively. No changes between the two groups were detected in the levels of total soluble tau, or its isoforms phosphorylated at Ser202/Thr205, Thr181, and Ser396/Ser404 as detected by HT7, AT8, AT270 and PHF1 antibodies, respectively (Figure 2B, C). These findings were confirmed by immunohistochemistry analysis of brain sections from the two groups of mice (Figure 3D). Next, we observed that

brain homogenates from the DIET group showed significantly higher level of formic acid-soluble tau fraction when compared to the control group (Figure 2E, F). To investigate the mechanism responsible for the changes in tau phosphorylation, we assessed the levels of some of the enzymes involved in its post-transcriptional regulation in the same tissues. As shown in figure 2G and H, while no changes between the two groups were observed for the steady state levels of cdk5, mice receiving the DIET manifested a significant increase in p35 and p25 levels, the activators of this very kinase when compared with controls. By contrast, no changes in total GSK3-α and GSK3-β, its phosphorylated forms, GSK3- α and -β (pGSK3-α/ β) and protein phosphatase 2A (PP2A) were observed between the two groups (Figure 2G, H). No significant differences were observed when males and females in each group were analyzed for any of these proteins separately (data not shown).

High homocysteine levels affect synaptic integrity and neuroinflammation

Next, we assessed the effect of high Hcy levels on synaptic integrity by measuring levels of a pre-synaptic integrity marker, synaptophysin (SYP), and a post-synaptic marker, post-synaptic protein 95 (PSD95), in the brains of the two groups of mice. Compared with controls, DIET-treated mice had a significant reduction in the steady state levels of PSD95, but no changes for the levels of SYP (Figure 3A, B). These results were confirmed by immunohistochemistry analysis (Figure 3C).

To measure neuroinflammation, brains from the two groups were assessed for levels of cluster of differentiation 45 (CD45), a marker of microglia activation, and the glial fibrillary acidic protein (GFAP), a marker of astrocyte activation. As shown in figure 3D and E, while no significant changes were observed between the two groups of mice for CD45 levels, we found that DIET-receiving mice had a statistically significant increment in the steady state levels of GFAP compared with control group. No significant differences were observed when males and females in each group were analyzed separately for both synaptic proteins and neuroinflammation (data not shown).

Elevated homocysteine levels upregulates 5LO pathway in the brain of h-tau mice

Since we previously demonstrated that high Hcy levels up-regulates the 5-lipoxygenase (5LO) pathway through demethylation of its promoter (11), next we wanted to see if this was also the case under our experimental condition. Compared with controls, mice with diet-induced high Hcy levels had a significant increase in the steady state levels of 5LO protein (Figure 4A, B). This increase was associated with a significant elevation of the enzymatic activity of the protein as shown by higher levels of the leukotriene B4 (LTB4), the major metabolic product of its activation (Figure 4C). Finally, we also measured the levels of 5LO mRNA in the same tissues and found that compared with controls, DIET-treated mice had a significant increase in its levels (Figure 4D). Coincidental with the changes in 5LO mRNA, we found that levels of DNA methyltransferase 1 (DNMT1) and DNMT3β were significantly reduced, but no differences in DNMT3α levels were detected between the two groups (Figure 4E, F). No significant differences were observed when males and females in each group were analyzed separately for any of these parameters (data not shown).

5LO upregulation precedes the high Hcy-dependent tauopathy phenotype

Next, we investigated whether 5LO upregulation occurred at the same time or before the tauopathy phenotype development upon diet-induced high Hcy levels in the same mice. To this aim, a separate group of tau transgenic mice was randomized to receive the DIET or regular chow for a shorter time period, from 4 to 8 months of age. Animals were later tested for cognitive performance, 5LO expression, and tau phosphorylation. After 4 months on the DIET, compared with controls h-tau mice did not manifest any significant changes in cognitive performance as assessed by Y-maze and Morris water maze test (data not shown). In a similar manner, we were not able to detect any significant changes in the levels of total soluble tau, its phosphorylated isoforms, and the insoluble fraction (Figure 5B–E). By contrast, the treatment resulted in higher levels of Hcy, and SAH and lower levels of SAM compared to controls (Figure 5A), and a significant increase in the steady state levels of 5LO proteins and its metabolic product, LTB4, compared to controls (Figure 5F–H).

Hcy-dependent 5LO activation regulates tau phosphorylation

To further support the direct role of Hcy in modulating tau phosphorylation via activation of the 5LO pathway, we treated neuroblastoma cells stably expressing human tau (N2A h-tau) with vehicle (CTR) or homocysteine (Hcy) (50 μM) in the presence or the absence of zileuton (100 μM), a specific 5LO inhibitor (20). This concentration of zileuton used is known to significantly suppress 5LO activation in vitro (20, 21). After 24hrs incubation, cell lysates were harvested for biochemistry analyses. A shown in figure 6, we observed that cells incubated with Hcy had a significant increase of tau phosphorylated at Thr231/Ser235 and Ser396, as recognized by AT180 and PHF13 antibodies, respectively. However, no changes were detected in the levels of total tau or its phosphorylated isoform at Thr181, as detected by HT7 and PHF1 antibodies respectively. Moreover, Hcy-treated cells showed higher levels of p35 and p25 but no change in total levels of cdk5 compared to CTR cells (Figure 6C, D). While zileuton alone di not induce significant changes in any of the different parameters described above, we found that it was able to completely prevent the effects that Hcy had on tau phosphorylation as well as p35 and p25 levels (figure 6A–D).

DISCUSSION

In the current study we report for the first time on the biological effect that diet-induced high Hcy levels *in vivo* has on the development of the entire tau pathological phenotype in a transgenic mouse model of human tauopathy. In particular, we demonstrate that chronic administration of a diet low in folate and B vitamins by increasing Hcy levels within the central nervous system directly up-regulates the 5LO enzymatic pathway which then promotes tau phosphorylation, synaptic pathology, neuroinflammation, and behavioral deficits in the h-tau transgenic mice.

In recent years, despite some conflicting results several epidemiological studies and cross-sectional clinical investigations have reported on the association between elevated Hcy levels and AD, suggesting that high Hcy is a metabolic risk factor for the disease and that its effect on AD pathogenesis is independent from other confounders (22–26). In support of these findings, experimental studies using mouse models of neurodegeneration and AD-like brain

amyloidosis have all shown that genetic or diet-induced high Hcy level results in a worsening of the AD-like phenotype, by promoting Aβ accumulation in the brain parenchyma and the vasculature (27–29). Interestingly, we reported that besides Aβ a condition of elevated HCy levels can also influence tau phosphorylation suggesting a possible role of this risk factor in tau metabolism (30). Although in vitro we showed that blocking Aβ production with a gamma-secretase inhibitor did not influence tau phosphorylation, considering the data showing that in vivo Aβ can influence tau pathology, in those studies we could not rule out that the in vivo effect seen on tau was secondary to the changes in Aβ levels (13, 30).

To prove a direct role of Hcy on tau phosphorylation in vivo we embarked in the current study in which we used a well-established dietary approach, consisting in the chronic administration of a diet low in folate and B vitamins, which is known to result in higher Hcy levels. The diet was administered to a relevant mouse model of pure tauopathy, which displays age dependent memory impairments, synaptic dysfunction and pathology, as well as progressive accumulation of hyper-phosphorylated tau protein and importantly devoided of any Aβ pathology (31).

Initially, we observed that after 6 months on the diet the tau transgenic mice had significant impairments of their spatial and learning abilities in the Morris water maze as demonstrated by the longer time during the training phase that took them to reach the platform when compared with controls. This impairment was also evident during the probe phase of the test in which we observed that compared with controls the DIET-treated mice had a lower number of entries and time spent in the platform zone, and a higher time spent in the opposite quadrant. Having observed significant memory and learning impairments resulting from the DIET, we next assessed whether the same experimental treatment had an effect on tau phosphorylation. First, we found that there were no differences in the levels of soluble tau protein when we compared the two groups of mice, suggesting that the treatment did not have any effect on the tau transgene. By contrast, DIET-treated h-tau mice showed a significant increase in the levels of phosphorylated tau isoforms at two specific epitopes, Thr231/Ser235 and Ser396, when compared with the control group. Since in this mouse model it is known that with age the mice develop also discrete deposits of the insoluble forms of the tau protein, we were every interested in assessing their brains for this aspect of the tau pathological phenotype. At the end of the treatment we observed that mice with diet-induced high Hcy levels in the central nervous system had a significant elevation of the insoluble tau fraction in their brain tissues.

In an effort aimed at elucidating potential mechanisms responsible for these changes in tau phosphorylation and solubility, we assessed some of the recognized kinases as important modulators of this aspect of tau neurobiology. While we did not observe any changes in levels of total and phosphorylated GSK3α and GSK3β, we found that the diet group had a significant increase in the two major activators of the cdk5 kinase when compared with control mice, supporting a functional role for this kinase pathway in the biological effect on tau. In addition, analysis of biochemical markers of synaptic integrity revealed that mice chronically receiving the DIET had significant reduction in the levels of PSD95, which is in

line with the behavioral deficits we observed during the execution and analysis of the Morris water maze results.

Since our recent work has demonstrated that high Hcy levels by reducing the levels of the major enzymes responsible for the *de novo* DNA methylation promotes 5LO upregulation, we wanted to see if this was also the case under our experimental conditions (32). Analyses of brain tissues from h-tau mice receiving the DIET showed that indeed they had a significant increase in the steady state levels of 5LO protein as well as its enzymatic activity and its mRNA levels. Confirming our previous work, these changes were associated with a significant reduction in the methyl transferase enzymes in the same samples, supporting an epigenetic modification of the 5LO pathway secondary to the elevated Hcy condition.

To investigate whether the changes in the 5LO were primary or secondary to the development of the tau neuropathological phenotype, we treated a separate group pf h-tau mice for a shorter time: 4 months. At the end of this trial, we observed no significant changes in terms of behavior, tau phosphorylation, and astrocyte activation between the DIET-treated and controls. By contrast, we found that compared with the control group transgenic mice receiving the DIET had a significant increase in brain Hcy levels together with an up-regulation of the 5LO enzymatic pathway. Taken together these data support the novel hypothesis that 5LO activation is an earlier event in the elevated Hcy-dependent development of the tau neuropathological phenotype in this model of tauopathy.

To further prove the biological link between HHcy-induced tau phosphorylation and 5LO upregulation we implemented an in vitro cellular system which recapitulates our mouse model, neuronal cells stably expressing all six human tau isoforms. Cells incubated with Hcy had a significant increase in 5LO as well as tau phosphorylation at the same epitopes as in the *in vivo* and an activation of the cdk5 kinase pathway. However, these biological effects were competed prevented if together with the Hcy cells were incubated with a specific and irreversible 5LO inhibitor, suggesting a necessary role of this enzyme for the Hcy-dependent effect on tau phosphorylation.

While there is an apparent discrepancy between the timeline of the in vivo versus the in vitro results, with the former taking up to 8 months to observe the effect on the tau pathological phenotype and the latter only 24 hrs, we need to consider that it is always very difficult to simply compare these two settings. We believe that the complexity of the whole animal biology system, which contains a combination of different cell types and biological environment in most of the cases should be considered responsible for those apparent differences.

In conclusion, our studies represent the first experimental evidence showing that elevated HCy levels within the central nervous system directly modulates tau phosphorylation, synaptic pathology, behavioral deficits and neuroinflammation by an up-regulation of the 5LO enzymatic pathway in a relevant mouse model of human tauopathy. They support the novel concept that high HCy levels should be considered as a metabolic risk factor also for human tauopathies, a group of neurodegenerative diseases characterized primarily by the progressive accumulation of highly phosphorylated tau protein.

Acknowledgments

The work presented in this paper was in part supported by grants from the National Institute of Health (HL112966, AG51684), and the Wanda Simone Endowment for Neuroscience.

References

1. Alzheimer's Association. 2016 Alzheimer's disease facts and figures. Alzheimer's Dement. 2016; 12(4):459–509. [PubMed: 27570871]
2. Giannopoulos, PG, Praticò, D. Alzheimer's disease. Diet and Nutrition in Dementia and Cognitive Decline. Martin, Colin R, Reddy, Victor, editors. Elsevier Publisher; London, UK: 2005. 13–21.
3. Arendt T, Stieler JT, Holzer M. Tau and tauopathies. Brain Res Bull. 2016; 126(Pt 3):238–292. [PubMed: 27615390]
4. Spillantini MG, Goedert M. Tau pathology and neurodegeneration. Lancet Neurol. 2013; 12(6):609–622. [PubMed: 23684085]
5. Smith AD, Refsum H. Homocysteine, B vitamins, and cognitive impairment. Annu Rev Nutr. 2016; 36:211–239. [PubMed: 27431367]
6. Shen L, Ji HF. Associations between homocysteine, folic Acid, vitamin B12 and Alzheimer's disease: insights from meta-analyses. J Alzheimers Dis. 2015; 46(3):777–790. [PubMed: 25854931]
7. Zhuo JM, Portugal GS, Kruger WD, Wang H, Gould TJ, Praticò D. Diet-induced hyperhomocysteinemia increases amyloid-beta formation and deposition in a mouse model of Alzheimer's disease. Curr Alzheimer Res. 2010; 7(2):140–149. [PubMed: 19939226]
8. Fuso A, Nicolia V, Ricceri L, Cavallaro RA, Isopi E, Mangia F, et al. S-adenosylmethionine reduces the progress of the Alzheimer-like features induced by B-vitamin deficiency in mice. Neurobiol Aging. 2012; 33(7):1482e1–16.
9. Zhuo JM, Praticò D. Normalization of hyperhomocysteinemia improves cognitive deficits and ameliorates brain amyloidosis of a transgenic mouse model of Alzheimer's disease. FASEB J. 2010; 24(10):3895–3902. [PubMed: 20519634]
10. Suszyńska-Zajczyk J, Luczak M, Marczak L, Jakubowski H. Hyperhomocysteinemia and bleomycin hydrolase modulate the expression of mouse brain proteins involved in neurodegeneration. J Alzheimers Dis. 2014; 40(3):713–26. [PubMed: 24496069]
11. Li JG, Barrero C, Merali S, Praticò D. Homocysteine modulates 5-lipoxygenase expression level via DNA methylation. Aging Cell. 2017; 16(2):273–280. [PubMed: 27896923]
12. Andorfer C, Kress Y, Espinoza M, de Silva R, Tucker KL, Barde YA, et al. Hyperphosphorylation and aggregation of tau in mice expressing normal human tau isoforms. J Neurochem. 2003; 86(3): 582–590. [PubMed: 12859672]
13. Li JG, Chu J, Barrero C, Merali S, Praticò D. Homocysteine exacerbates β-amyloid pathology, tau pathology, and cognitive deficit in a mouse model of Alzheimer disease with plaques and tangles. Ann Neurol. 2014; 75(6):851–863. [PubMed: 24644038]
14. Di Meco A, Lauretti E, Vagnozzi AN, Praticò D. Zileuton restores memory impairments and reverses amyloid and tau pathology in aged Alzheimer's disease mice. Neurobiol Aging. 2014; 35(11):2458–2464. [PubMed: 24973121]
15. Giannopoulos PF, Chu J, Sperow M, Li JG, Yu WH, Kirby LG, et al. Gene knockout of 5-lipoxygenase rescues synaptic dysfunction and improves memory in the triple-transgenic model of Alzheimer's disease. Mol Psychiatry. 2014; 19(4):511–518. [PubMed: 23478745]
16. Vagnozzi AN, Giannopoulos PF, Praticò D. The direct role of 5-lipoxygenase on tau pathology, synaptic integrity and cognition in a mouse model of tauopathy. Transl Psychiatry. 2017; 7(12): 1288. [PubMed: 29249809]
17. Giannopoulos PF, Chu J, Sperow M, Li JG, Yu WH, Kirby LG, et al. Pharmacologic inhibition of 5-lipoxygenase improves memory, rescues synaptic dysfunction, and ameliorates tau pathology in a transgenic model of tauopathy. Biol Psychiatry. 2015; 78(10):693–701. [PubMed: 25802082]
18. Moncada CA, Clarkson A, Perez-Leal O, Merali S. Mechanism and tissue specificity of nicotine-mediated lung S-adenosylmethionine reduction. J Biol Chem. 2008; 283(12):7690–7696. [PubMed: 18180293]

19. Joshi YB, Giannopoulos PF, Chu J, Sperow M, Kirby LG, Abood ME, et al. Absence of ALOX5 gene prevents stress-induced memory deficits, synaptic dysfunction and tauopathy in a mouse model of Alzheimer's disease. Hum Mol Genet. 2014; 23(25):6894–6902. [PubMed: 25122659]
20. Chu J, Giannopoulos PF, Ceballos-Diaz C, Golde TE, Praticò D. 5-Lipoxygenase gene transfer worsens memory, amyloid, and tau brain pathologies in a mouse model of Alzheimer disease. Ann Neurol. 2012; 72(3):442–454. [PubMed: 23034916]
21. Chu J, Praticò D. Pharmacologic blockade of 5-lipoxygenase improves the amyloidotic phenotype of an Alzheimer's disease transgenic mouse model involvement of γ-secretase. Am J Pathol. 2011; 178(4):1762–1769. [PubMed: 21435457]
21. Chu J, Praticò D. 5-Lipoxygenase pharmacological blockade decreases tau phosphorylation in vivo: involvement of the cyclin-dependent kinase-5. Neurobiol Aging. 2013; 34(6):1549–1554. [PubMed: 23332172]
22. McCully KS. Homocysteine metabolism, atherosclerosis, and diseases of aging. Compr Physiol. 2015; 6(1):471–505. [PubMed: 26756640]
23. Miwa K, Tanaka M, Okazaki S, Yagita Y, Sakaguchi M, Mochizuki H, et al. Increased total homocysteine levels predict the risk of incident dementia independent of cerebral small-vessel diseases and vascular risk factors. J Alzheimers Dis. 2016; 49(2):503–513. [PubMed: 26484913]
24. Aisen PS, Schneider LS, Sano M, Diaz-Arrastia R, van Dyck CH, Weiner MF, et al. High-dose B vitamin supplementation and cognitive decline in Alzheimer disease: a randomized controlled trial. JAMA. 2008; 300(15):1774–1783. [PubMed: 18854539]
25. Pratico D. High-dose B vitamin supplements and Alzheimer disease. JAMA. 2009; 301(10):1020–1021. [PubMed: 19278942]
26. Zhuo JM, Wang H, Praticò D. Is hyperhomocysteinemia an Alzheimer's disease (AD) risk factor, an AD marker, or neither? Trends Pharmacol Sci. 2011; 32(9):562–571. [PubMed: 21684021]
27. Pacheco-Quinto J, Rodriguez de Turco EB, DeRosa S, Howard A, Cruz-Sanchez F, Sambamurti K, et al. Hyperhomocysteinemic Alzheimer's mouse model of amyloidosis shows increased brain amyloid beta peptide levels. Neurobiol Dis. 2006; 22(3):651–656. [PubMed: 16516482]
28. Chung YC, Kruyer A, Yao Y, Feierman E, Richards A, Strickland S, et al. Hyperhomocysteinemia exacerbates Alzheimer's disease pathology by way of the β-amyloid fibrinogen interaction. J Thromb Haemost. 2016; 14(7):1442–52. [PubMed: 27090576]
29. Li JG, Praticò D. High levels of homocysteine results in cerebral amyloid angiopathy in mice. J Alzheimers Dis. 2015; 43(1):29–35. [PubMed: 25061050]
30. Li JG, Merali S, Pratico D. Five lipoxygenase hypomethylation mediates the homocysteine effect on Alzheimer's phenotype. Sci Rep. 2017; 6(7):46002.
31. Polydoro M, Acker CM, Duff K, Castillo PE, Davies P. Age-dependent impairment of cognitive and synaptic function in the htau mouse model of tau pathology. J Neurosci. 2009; 29(34):10741–10749. [PubMed: 19710325]
32. Li JG, Barrero C, Merali S, Praticò D. Genetic absence of ALOX5 protects from homocysteine-induced memory impairment, tau phosphorylation and synaptic pathology. Hum Mol Genet. 2017; 26(10):1855–1862. [PubMed: 28334897]

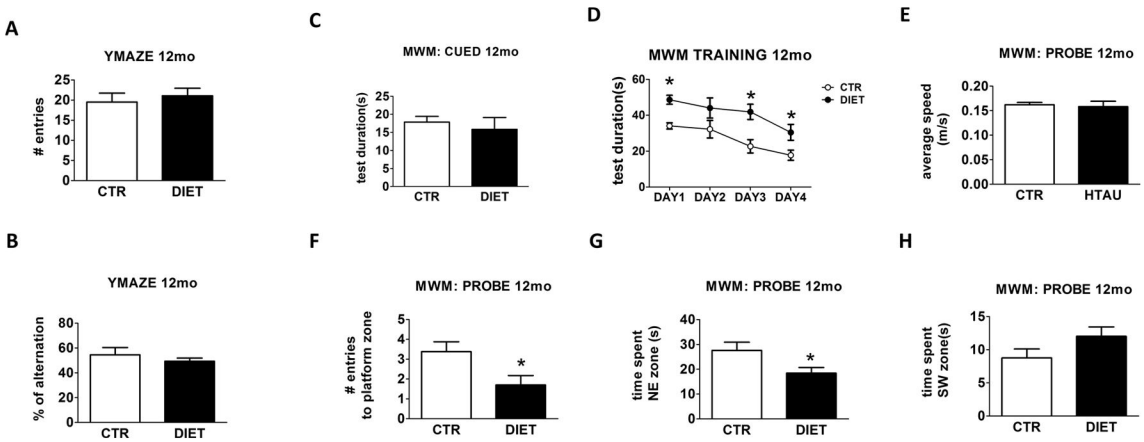

Figure 1. Diet low in folate and B vitamins induces behavioral deficits

Starting at 4 month of age h-tau mice were randomized to receive a low folate and B 12 vitamin diet (DIET), or regular chow diet (CTR) for 8 months then assessed in the Y-maze and the Morris water maze. **A**. Number of total arm entries for mice receiving the DIET or regular chow (CTR). **B**. Percentage of alternations between h-tau mice receiving the DIET or regular chow (CTR). **C**. Morris water maze cued response of h-tau mice receiving DIET or controls (CTR). **D**. Four days training for the same two groups of mice. **E**. Average swim speed for the two groups of mice, DIET and CTR. **F**. Number of entries to the target platform zone for h-tau receiving the DIET or chow diet control (CTR). **G**. Time in the NE target platform zone for the same two groups of mice, DIET and CTR **H**. Time spent in the opposite zone for the same two groups of mice, DIET and CTR (* $p < 0.05$) (n=8 CTR, n=10 DIET). Values represent mean ± sem.

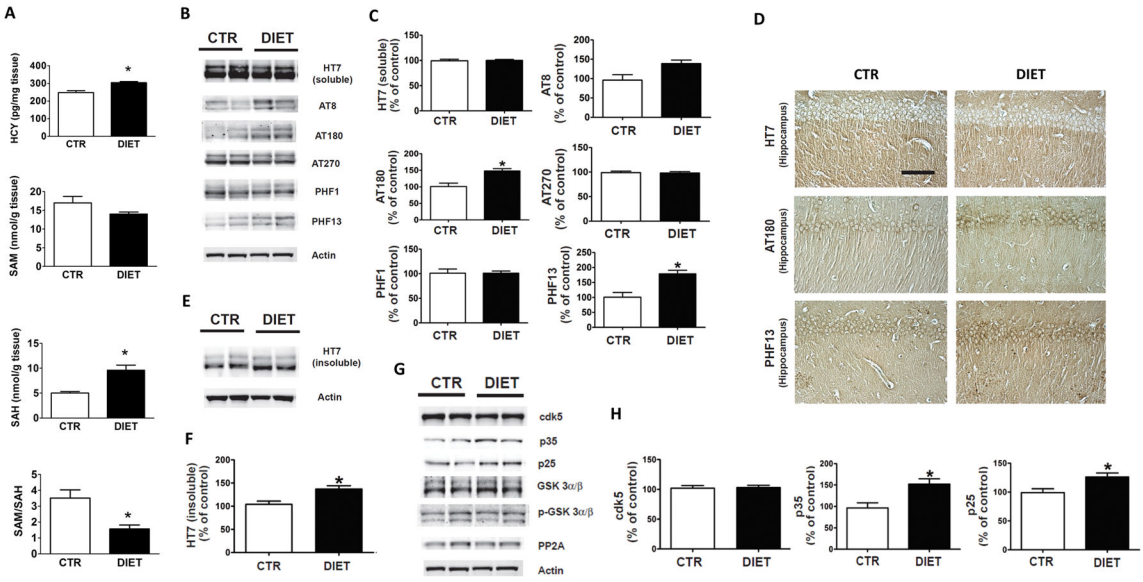

Figure 2. Diet-induced HHcy in brain affects tau phosphorylation and pathology

A. Brain cortex homogenates from h-tau mice receiving the low folate and B vitamins diet (DIET) or chow diet controls (CTR) from 4 to 12 months of age were assayed by HPLC for levels of Hcy, SAM, SAH, and the ratio SAM/SAH calculated (*p<0.05) (n=5 per group). **B**. Representative Western blots of soluble total tau protein (HT7), phosphorylated tau at residues Ser202/Thr205 (AT8), Thr231/Ser235 (AT180), at Thr181 (AT270), Ser396/Ser404 (PHF1) and Ser396 (PHF13) in brain cortex homogenates from h-tau mice receiving the DIET or regular chow from 4 to 12 months of age. **C**. Densitometric analyses of the immunoreactivities to the antibodies shown in the previous panel. **D.** Representative images of brain sections from DIET-treated or controls (CTR) h-tau mice immunostained with HT7, AT180, and PHF13 antibodies (Scale bar: 100μm). **E.** Representative Western blot for formic acid soluble (insoluble) total tau (HT7) protein in brain cortex homogenates from the same two groups of h-tau mice. **F**. Densitometric analyses of the immunoreactivities to the antibody shown in the previous panel. **G**. Representative Western blots of cdk5, p35, p25, GSK3α, GSK3β, p-GSK3α, p-GSK3β, and PP2A in brain cortex homogenates from the same two groups of h-tau mice, CTR ad DIET. **H.** Densitometric analyses of the immunoreactivities to the antibodies shown in the previous panel (* p< 0.05), (n=4 CTR, n=4 DIET). Values represent mean ± sem.

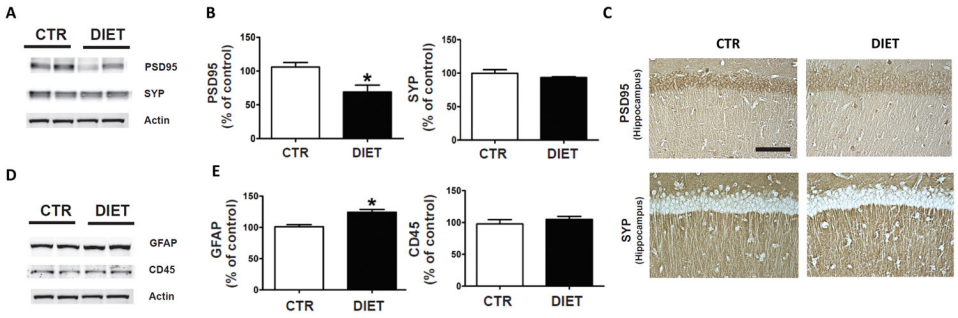

Figure 3. Diet-induced HHcy affects synaptic integrity and neuroinflammation

A. Representative Western blot analyses of post-synaptic density protein 95 (PSD95) and synaptophysin (SYP) in brain cortex homogenates of mice receiving the DIET or regular chow from 4 to 12 months of age. **B**. Densitometric analyses of the immunoreactivities to the antibodies shown in the previous panel. **C**. Representative images of brain sections from the same two groups of h-tau mice, CTR ad DIET, immunostained with PDS95 and synaptophysin antibodies (Scale bar: 100μm). **D**. Representative Western blots of GFAP and CD45 in brain cortex homogenates from the same two groups of h-tau mice, CTR ad DIET. **E**. Densitometric analyses of the immunoreactivities to the antibodies shown in the previous panel (* $p < 0.05$), (n=4 CTR, n=4 DIET). Values represent mean ± sem.

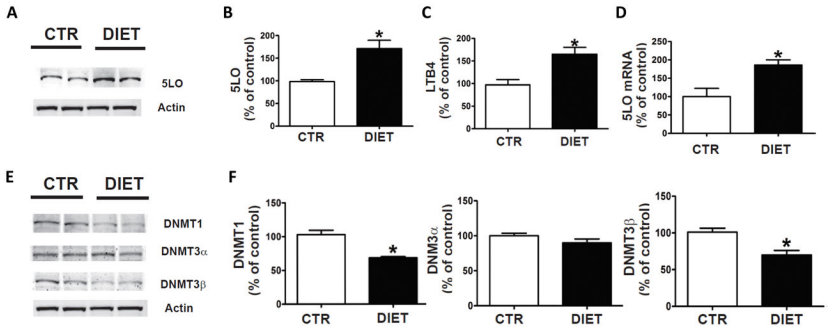

Figure 4. Diet-induced HHcy upregulates 5LO enzymatic pathway

A. Representative Western blot analysis of 5LO protein in brain cortex homogenates from h-tau mice receiving regular chow (CTR), or folate and B vitamins deficient diet (DIET) from 4 to 12 months of age. **B.** Densitometric analysis of the immunoreactivity to the antibody shown in the previous panel. **C.** Levels of LTB4 measured by a specific and sensitive ELISA assay in brain cortex homogenates from the same two groups of h-tau mice. **D.** Quantitative real time Reverse Transcription Polymerase Chain Reaction (q RT-PCR) analysis of 5LO mRNA in brain cortices of same two groups of h-tau mice, CTR ad DIET. **E.** Representative western blot analyses for DNMT1, DNMT3α, and DNMT3β in brain cortices of the same two groups of mice. **F.** Densitometric analyses of the immuno-reactivity to the antibodies shown in the previous panel (* $p < 0.05$) (n=4 CTR, n=4 DIET). Values represent mean± s.e.m.

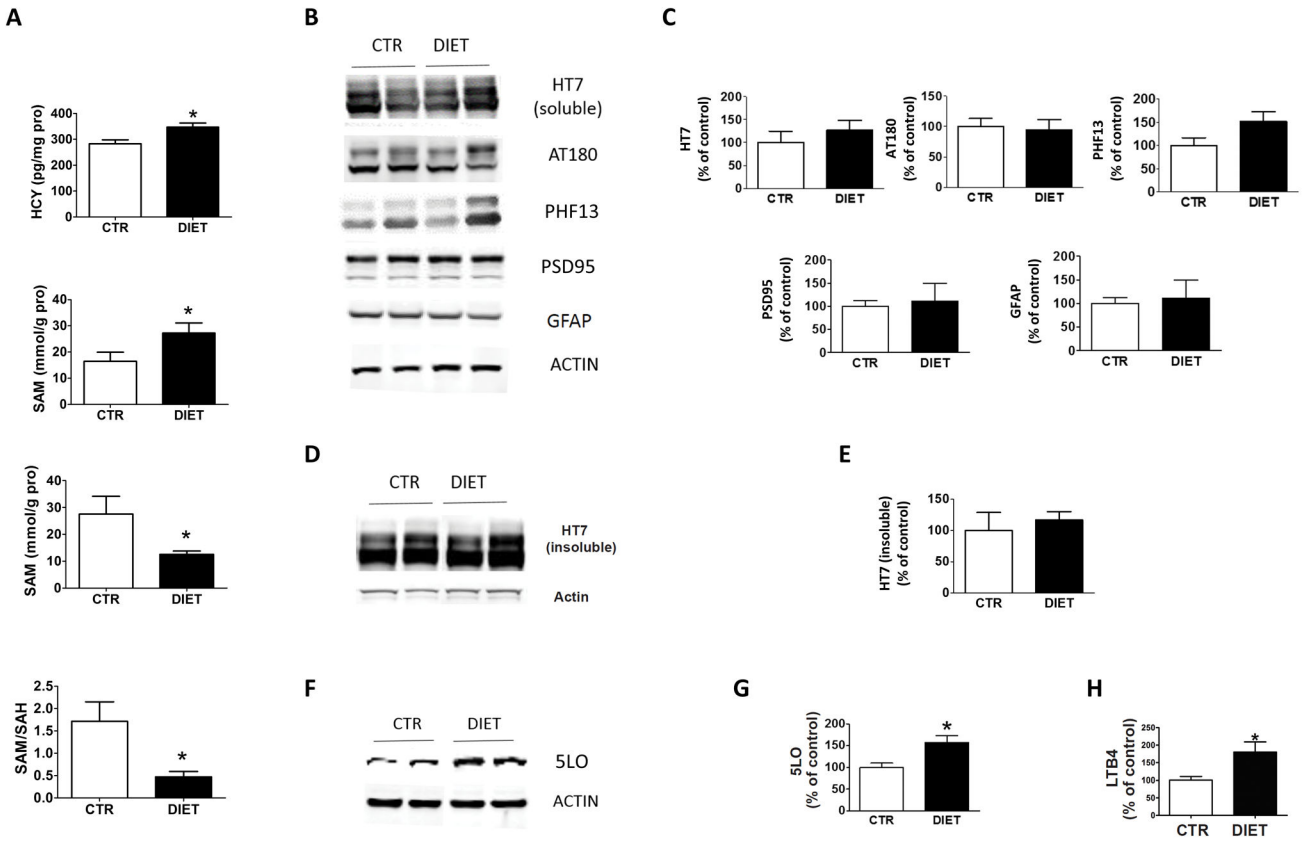

Figure 5. Diet induced HHcy-dependent 5LO upregulation precedes tau pathological phenotype

A. Brain cortex homogenates from h-tau mice receiving the low folate and B vitamins diet (DIET) or chow diet controls (CTR) from 4 to 8 months of age were assayed by HPLC for levels of Hcy, SAM, SAH, and the ratio SAM/SAH. **B.** Representative western blot analysis of soluble total tau protein (HT7), phosphorylated tau at residues Thr231/Ser235 (AT180) and Ser396(PHF13), post-synaptic density protein 95 (PSD95) and GFAP in brain cortex homogenates from h-tau mice receiving the DIET or regular chow from 4 to 8 months of age. **C.** Densitometric analysis of the immunoreactivity to the antibody shown in the previous panel. **D.** Representative western blot for formic acid soluble (insoluble) total tau (HT7) protein in brain cortex homogenates from the same two groups of h-tau mice, CTR ad DIET. **E.** Densitometric analyses of the immunoreactivities to the antibody shown in the previous panel. **F.** Representative western blot analysis of 5LO protein in brain cortex homogenates from the same two groups of h-tau mice, CTR ad DIET. **G.** Densitometric analysis of the immunoreactivity to the antibody shown in the previous panel. **H.** Levels of LTB4 measured by a specific and sensitive ELISA assay in brain cortex homogenates from the same two groups of h-tau mice (*$p < 0.05$ (n=4 CTR, n=4 DIET). Values represent mean ± s.e.m.

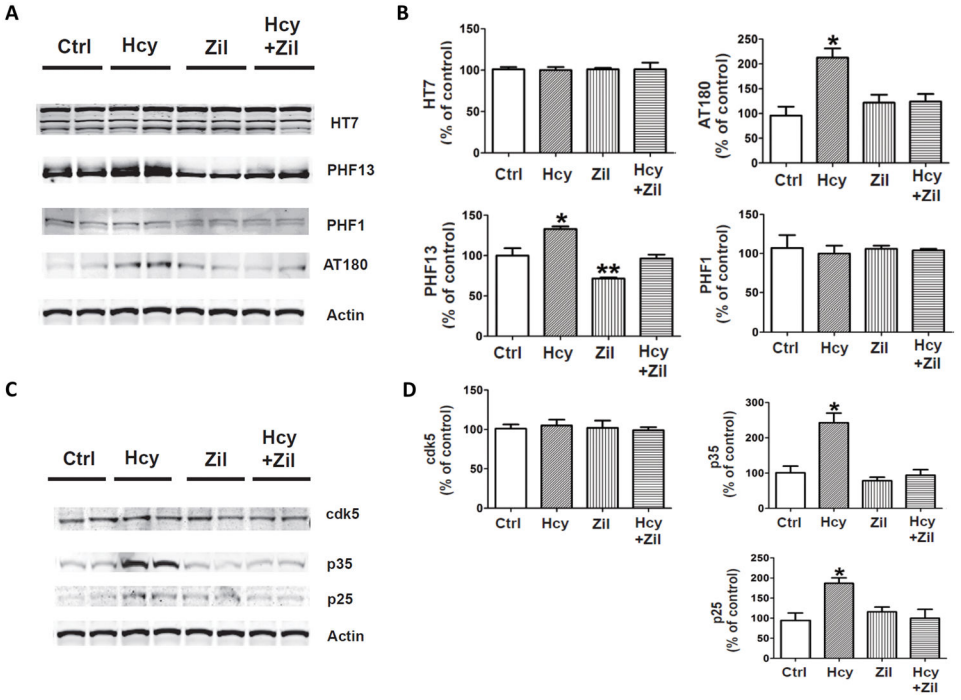

Figure 6. HHcy effect on tau phosphorylation is 5LO-dependent

N2A neuronal cells stably expressing human tau were incubated for 24hrs with Hcy (50μM) in the presence or absence of zileuton (100μM), then cells harvested for biochemistry analyses. **A**. Representative western blots of total tau (HT7), phosphorylated tau at residues Thr231/Ser235 (AT180), Ser396/Ser404 (PH1), and Ser396 (PHF13) in lysates from cells incubated with Hcy (HCY), vehicle (CTR), zileuton, or zileuton plus Hcy. **B**. Densitometric analyses of the immunoreactivities to the antibodies shown in the previous panel. **C**. Representative western blots of cdk5, p35, and p25 in lysates from cells incubated with Hcy (HCY), vehicle (CTR), zileuton alone, or zileuton plus Hcy. **D**. Densitometric analyses of the immunoreactivities to the antibodies shown in the previous panel (*$p < 0.05$)(n=4 per codition). Values represent mean ± sem.

Table 1

Antibodies used in the study.

Antibody	Immunogen	Host	Application	Source	Catalog Number
HT7	aa 159-163 of human tau	Mouse	WB, IHC	Thermo	MN1000
AT8	Peptide containing phospho-S202/T205	Mouse	WB	Thermo	MN1020
AT180	Peptide containing phospho-T231/S235	Mouse	WB, IHC	Thermo	P10636
AT270	Peptide containing phospho-T181	Mouse	WB	Thermo	MN1050
PHF13	Peptide containing phospho-Ser396	Mouse	WB, IHC	CST	9632
PHF1	Peptide containing phospho-Ser396/S404	Mouse	WB	Dr. Davies	Gift
cdk5	Cyclin-dependent kinase 5	Mouse	WB	Santa Cruz	sc-249
p35/25	Cyclin-dependent kinase 5 activator 1	Rabbit	WB	Santa Cruz	sc-820
GSK3α/β	Glycogen Synthase Kinase 3 alpha/beta	Mouse	WB	Santa Cruz	sc-56913
p-GSK3α/β	phospho-Glycogen Synthase Kinase 3 alpha/beta	Rabbit	WB	CST	9331
PP2A	Protein Phosphatase 2A	Rabbit	WB	Thermo	PA5-17510
PSD95	Purified recombinant rat PSD-95	Mouse	WB, IHC	Thermo	MA1-045
SYP	aa 221-313 of SYP of human origin	Mouse	WB, IHC	Santa Cruz	sc-55507
GFAP	spinal cord homogenate bovine origin	Mouse	WB	Santa Cruz	sc-33673
CD45	aa 1075-1304 of CD45 human origin	Rabbit	WB	Santa Cruz	sc-25590
5LO	Human 5-Lipoxygenase aa. 442-590	Mouse	WB	BD Transduction Laboratories	610695
DNMT1	aa 1317-1616 mapping near the C-terminus of Dnmt1 of human origin	Rabbit	WB	Santa Cruz	sc-20701
DNMT3α	aa 1-295 of Dnmt3α of human origin	Rabbit	WB	Santa Cruz	sc-20703
DNMT3β	aa 1-230 mapping near the N-terminus of Dnmt3β of human origin	Rabbit	WB	Santa Cruz	sc-20704
Actin	gizzard Actin of avian origin	Mouse	WB	Santa Cruz	sc-47778

WB: Western blot; IHC: immunohistochemistry.

Mol Psychiatry. Author manuscript; available in PMC 2019 October 26.